VII Brazilian Symposium on Rock Mechanics – SBMR 2016
Rock Mechanics and Rock Engineering for Innovation and Development
ISRM Specialized Conference 19-22 October, Belo Horizonte, Minas Gerais, Brazil

Effects of Fluid Confinement on Poor Quality Cemented Wellbores through Salt Formations

Daniel Duque Estrada Fernandes de Melo
GTEP PUC-Rio, Rio de Janeiro, Brazil, danielduquemelo@puc-rio.br

Juan David V. Uribe
GTEP PUC-Rio, Rio de Janeiro, Brazil, juandavid@puc-rio.br

Sérgio A. B. da Fontoura
GTEP PUC-Rio, Rio de Janeiro, Brazil, fontoura@puc-rio.br

Nelson Inoue
GTEP PUC-Rio, Rio de Janeiro, Brazil, inoue@puc-rio.br

Jorel L. R. Anjos
Petrobrás, Rio de Janeiro, Brazil, jorel.anjos@petrobras.com.br

SUMMARY: Wells drilled through salt formations are a big challenge in oil industry. Due to Salt time dependent behavior, loads can significantly modify during long term production. In deep wells, high temperatures and high pressure lead to great deformations on annular volume due to well closure. In the annular above cemented region, near uniform loads on casing are expected due to its high volume. In the cemented region, its quality has a major role on wellbore integrity though. As reported in literature, the presence of non-uniform loads can significantly reduce critical pressure, leading to casing failure. Thus, to evaluate effects of cement quality on casing failure, two scenarios must be considered: 1) Cement fault connected to the whole annular, where fluid can migrate to annular above top of cement; and 2) Trapped mud pocket, where drilling mud is confined and no fluid scape to the rest of the annular. The present study consists on a parametric finite element analysis of 10%, 20%, 30% and 40% defects on cemented annular based on a plane strain analysis. For the simulation, both fluid compressibility and thermal expansion are computed with the use of fluid elements. In the model with connected cement fault, fluid pressure is determined based only on its density. For the confined cement flaw, pressure may increase based on casing and salt deformation over the mud pocket volume. Results show that the span of cement fault on connected annular has a significant impact on casing stresses. For defects lower than 10%, casing stresses do not vary much. As defects increase, non-uniformity of load leads to significant casing deformation when the defects are connected to the annular above. If cement faults are confined, the fluid compliance significantly modifies system response though. As a function of fluid compressibility, the confinement tends to equilibrate pressure difference as casing deforms. Thus, the connectivity of defect cavity has a big impact on the well integrity.

KEYWORDS: Casing Failure, Mud Pocket, Non-Uniform Loads, Salt Creep.

1 INTRODUCTION

Besides ensuring wellbore stability, cementing operation has the goal of restricting fluid communication between different annulus and the borehole wall. The result of an unsuccessful cementing work is the generation of multiple spaces without cement or mud pockets (figure 1).

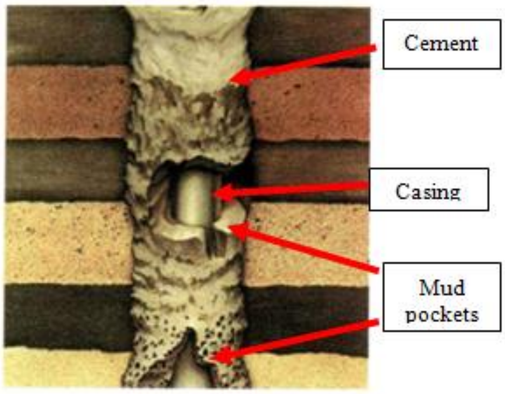

Figure 1. Well scheme with a mud pockets (Thomas, 2001).

Common consequences of ineffective cementing operations are: mud losses, uncontrolled fluids influx, difficulty in reservoir control and unsuccessful stimulation operations. For casing integrity purposes, mud pockets have a major impact on collapse resistance due to presence of non-uniform loads. In the presence of evaporites, there is also the annular pressure buildup effect (APB) where rock creep into cement flaw, which contribute to casing collapse.

According to Santos (2006) density, gelling and cement adherence are the main factors that influence a correct cementation. Poaite (2012) performed numerical simulations of a symmetric mud pocket analyzing mainly the casing yield index due to salt creep and a constant internal pressure. Mackay (2011) performed numerical simulations of drilling-cementing procedure in an oil well, analyzing the critical stresses in the casing. Zhang (2008) presents a 3D study of point loads in the casing due to salt creep. Jammer et al (2015) conducted a laboratory tests considering mud pockets with/without cement micro annuli on pipe-in-pipe system, comparing the results with numerical simulations.

The present study investigates effects of mud pocket span and its connectivity to the rest of the annular on casing failure. Based on parametric finite element simulations, cement flaws of 10%, 20%, 30% and 40% were analyzed, taking into account salt creep and fluid compressibility.

2 CONSTITUTIVE MODELS OF MATERIALS

In this section it will be presented the main mathematical laws to model the behavior of materials numerical simulations.

2.1 Salt

Salt rock has a time dependent behavior that leads to deformation over time for an constant applied differential load, as shown in Figure 2 for a sample under constant uniaxial stress. There are three creep stages: a) primary, characterized by an instantaneous elastic deformation followed by an increase of the strain rate over time; b) secondary, where a constant strain rate is expected; and c) tertiary, where strain rate increases up to the shear failure.

For a long term production, only the secondary creep stage is considered. At this stage, if the stress is suddenly reduced to zero, a recovery of the elastic strain occur, followed by a slow recovery over time.

The law adopted to model the creep behavior is the double mechanism creep law, as shown in Eq. (1) (Poiate and Costa, 2006). Based on laboratory tests, Figure 3 shows the secondary creep rate vs. differential stress curve for Halite, Carnalite and Taquidryte. It can be seen that above 10 MPa Halite and Taquihidryte present a non-linear relation to differential stress, leading to higher strain rates.

$$\dot{\varepsilon} = \dot{\varepsilon}_0 \left(\frac{\tilde{q}}{\sigma_0} \right)^n \exp\left(\frac{Q}{R\theta_0} - \frac{Q}{R\theta} \right) \quad (1)$$

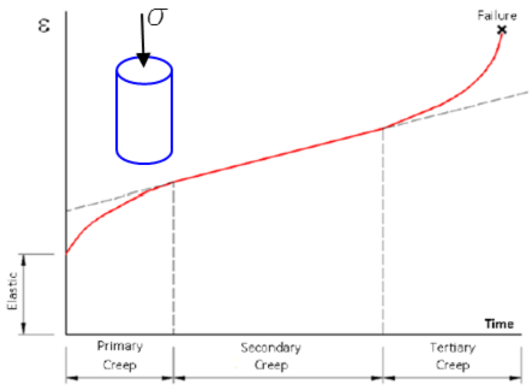

Figure 2. A typical creep behavior and its stages.

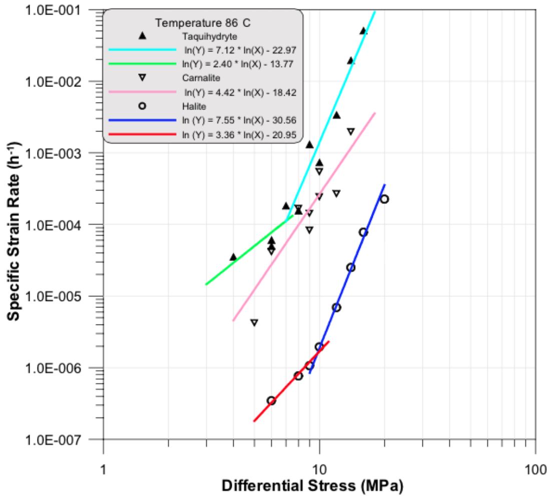

Figure 3. Creep rate as function of differential stress based on double mechanism creep law (Poiate and Costa, 2006).

2.2 Casing

Pipe strength is modeled through von Mises Yield criteria (Eq. 2), where the yield is independent of the confinement stresses.

$$\tilde{q} = \sqrt{\frac{(\sigma_1 - \sigma_2)^2 + (\sigma_1 - \sigma_3)^2 + (\sigma_2 - \sigma_3)^2}{2}} \qquad (2)$$

Figure 4 shows the von Mises yield surface in the principal stresses space, where points inside the surface represent the elastic behavior, and points at the surface are points that have reached the yield strength. If the material remains loaded above the yield point, a new surface (red) is generated due to material hardening, where irreversible strains are expected. Therefore, a larger load increment is required to yield material again, until it reaches the maximum resistance of material.

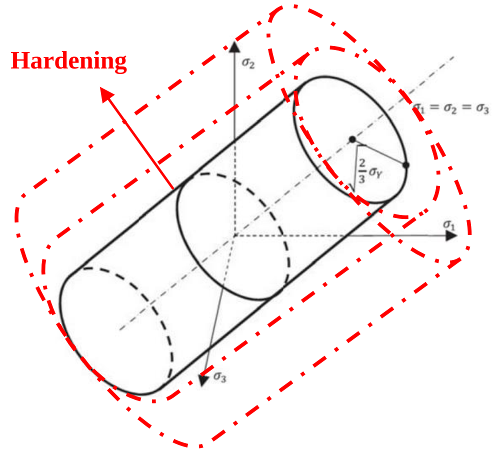

Figure 4. Von Mises yield surface in principal stresses space.

2.3 Fluid

Fluid compressibility is the compliance capability that relates the volume change with the fluid pressure. Accounting mud pocket's volume variation due to salt creep and fluid expansion, Eq. 3 is used.

$$\frac{\partial P}{\partial t} = -\frac{K}{V_0}\frac{\partial V}{\partial t} + \alpha K \frac{\partial \theta}{\partial t} \qquad (3)$$

Usually, fluid compressibility effects are neglected in conventional well simulations, but they are important since pressure variation can significantly change casing response. In scenarios of non-uniform loads, small pressure increase can equilibrate load difference over the pipe's wall. On the other hand, if the pressure increase is severe, it can lead to casing collapse.

3 CASING INTEGRITY ON POORLY CEMENTED WELLBORES

The analysis of casing integrity is based on parametric studies in order to investigate mud compressibility and salt creep effects over a mud pocket. Assuming a 2080 meters long salt section beneath 1290 meters sediments and 1900 meters of water depth, overburden stresses and geothermal temperature can be seen in Table 1.

The well configuration is a 17 ½" wellbore drilled with 12ppg mud weight. With the casing shoe set at 5270 meters depth and a 520 meters column of cement, it was analyzed the feasibility of a 14", 114lb/ft, P110 casing.

The simulations consist on a plane-strain analysis (Figure 5) near the top of cement (4770m), considering cement flaws of 10%, 20%, 30% and 40% of the annulus. Due to its proximity to annular above TOC, two hypothesis must be considered: 1) The flaw is connected to the whole annulus; and 2) The fluid is trapped inside the failure. In a connected cement flaw, since the annular above TOC is significantly larger than the flaw itself, no pressure increase is expected since the fluid can escape. On the other hand, in a confined space, wellbore closure and fluid expansion significantly increase fluid pressure as it tends to equilibrate overburden stress.

Table 1. Overburden and Temperature of Salt layer.

Depth (m)	Overburden (Mpa)	Temperature (°C)
3190	47.66	70.3
4770	79.48	84.5
5270	89.55	89

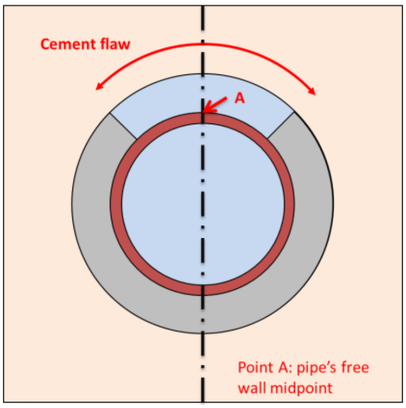

Figure 5. Plane strain simulation scheme.

For the safe dimensioning, casing internal pressure is assumed to be 5 MPa (Packer differential pressure failure) and open to surface, which leads to no compressibility effects in the interior of inner tube. In addition, since creep rates vary from different rock's chemical composition, two salts were investigated: 1) Low mobility Halite; and 2) High mobility Carnalite.

4 RESULTS

4.1 Connected Cement flaw

Assuming Halite and Carnalite creeping into a mud pocket connected to the whole annular, cement flaws of 10%, 20%, 30% and 40% were analyzed for the 14" casing.

Comparing pipe yield index, i.e., maximum von Mises stress to Yield stress ratio, it can be seen in Figures 6 and 7 that Carnalite's greater creep rate result in faster deformation, leading to faster load increase and higher stresses in a short term. In a long term, Halite's low creep rate and higher Young Modulus surpasses Carnalite related loads, generating higher overall stresses.

Due to salt creep, rock-pipe contact at pipe's free wall midpoint (Figure 5) occurs for defects equal (Carnalite) or greater (Halite and Carnalite) than 20%, counteracting localized bucking. For 20%, 30% and 40% defects and Carnalite, contact occurs at 3.6, 0.72 and 0.53 years, respectively. The sooner contact of greater defects lies on the lower stiffness of the rock near the mud pocket, being favorable to its mobility. Regarding Halite, pipe-rock contact only happens on 30% and 40% defects, at times of 8.3 and 10.8 years, respectively.

Although greater defect span, 40% flaw in Halite present later contact due to higher localized buckling on casing wall. Figure 8 shows a comparison of Halite and Carnalite deformation over 20% mud pocket.

For both rocks, defects of 30% are the ones that induce higher stresses in the pipe. The main reason is due to pipe's free wall length and buckling modes. From the solution of pipe stability, first and second order buckling modes are plotted in Figure 9 (Timoshenko and Gere, 1961). Since cement prevents pipe deformation, first mode buckling does not occur (pipe critical length equals half of its surface). The second order buckling mode occur at angles multiple of 45°, which represents critical length as a quarter of the pipe.

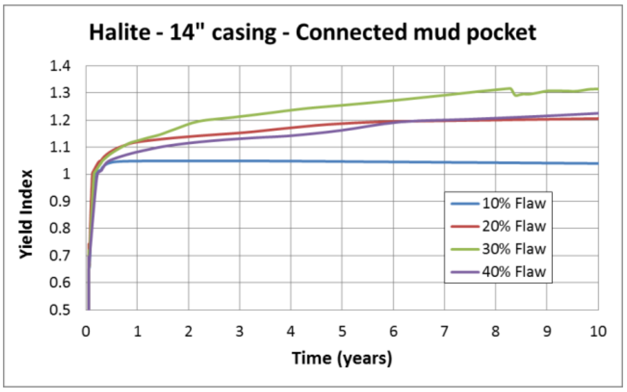

Figure 6. Yield index for 14” casing and Halite over time.

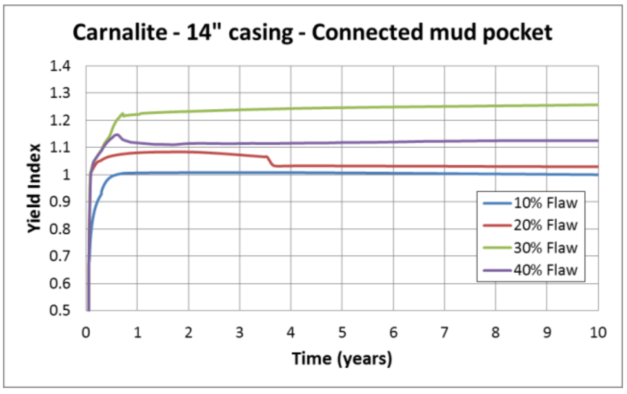

Figure 7. Yield index for 14” casing and Carnalite over time.

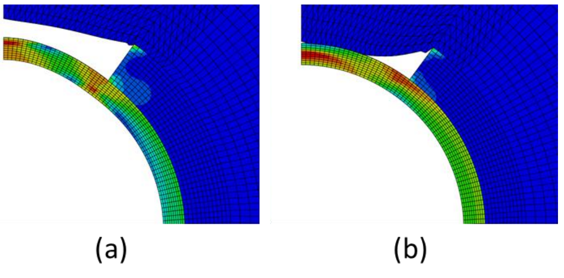

Figure 8. Comparison of rock deformation into 20% mud pocket for a) Halite and b) Carnalite.

Figure 10 shows casing and cement deformation for different cement flaws for Carnalite rock. For flaws of 10% and 20% span, pipe’s free wall is small, and so is its deformation. The increase of defect spans result in a free surface higher than the critical length for second mode buckling. Thus, due to pressure discontinuity at cement-fluid interface, high deformation happens. It is worth mentioning that for 40% defect the localized buckle is smaller than 30% flaws. This is associated with the rigid body displacement, which is expected for defects near or greater than half of the wellbore.

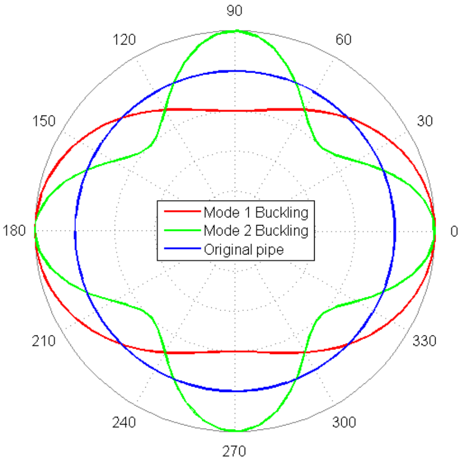

Figure 9. First two pipe buckling mode.

4.2 Effect of fluid confinement

Assuming Halite and Carnalite for cement flaws of 10%, 20%, 30% and 40%, 14” casing stresses are presented in Figures 11 and 12, respectively. The effect of fluid compressibility due to flaw’s volume reduction as salt creeps into it tend to equilibrate pressure on the defect with overburden stresses, generating an uniform load on casing wall.

Comparing yield index (maximum von Mises stress to Yield stress ratio), it can be seen that Carnalite’s higher creep rate and greater compliance tend to equilibrate loads on casing wall faster, transfering pressure increase to the rock and resulting in lower overall stresses.

Casing deformation and salt creep have an important role in load standardization. For mud pockets of 10%, neither salt creep nor casing deformation are significant, which result in relative low stresses.

For Halite (low creep rate), fluid initial pressurization happen mainly because of pipe displacement (rigid body) and deformation (buckling), that is more severe for greater defects. Therefore, greater defects result in faster load discontinuity reduction and lower stresses. It is important to mention that Halite has higher Young Modulus when compared to Carnalite. Thus, mud pocket pressure increase is transferred directly to the pipe, resulting in a magnitude greater than overburden stress (Figure 13).

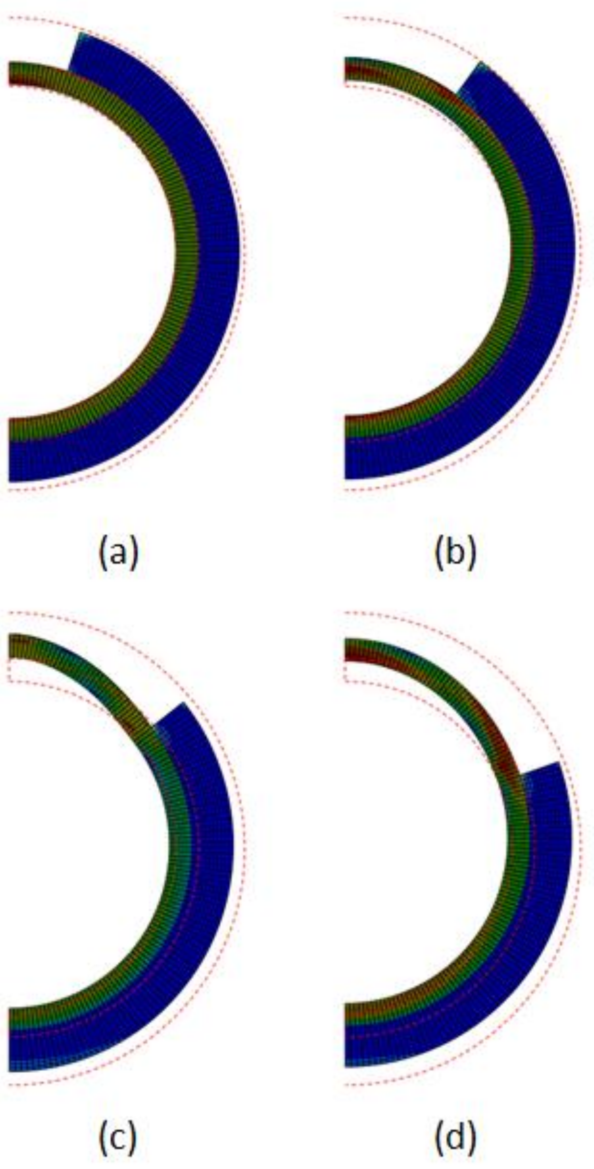

Figure 10. Comparison of casing and cement deformation for mud pocket of a) 10%, b) 20%, c) 30% and d) 40%, based on Carnalite rock.

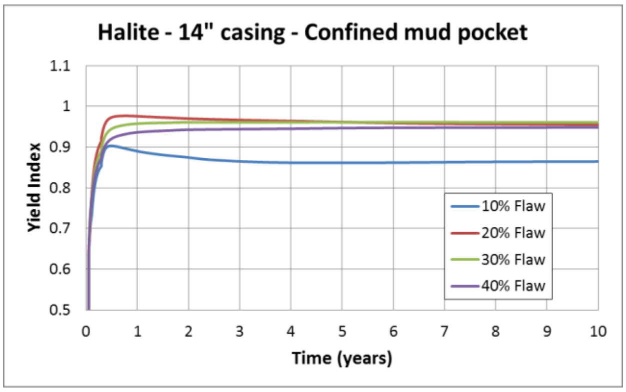

Figure 11. Yield index for 14" casing and Halite over time.

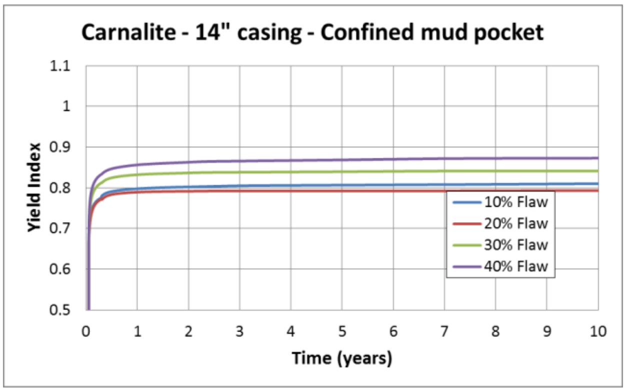

Figure 12. Yield index for 14" casing and Carnalite over time.

On the other hand, Carnalite tend to fill up mud pocket and reach equilibrium pressure faster. Since Carnalite is more compliant, any increase in fluid pressure will be transferred to the rock, and its relaxation equilibrates flaw's pressure with overburden stresses (Figure 14).

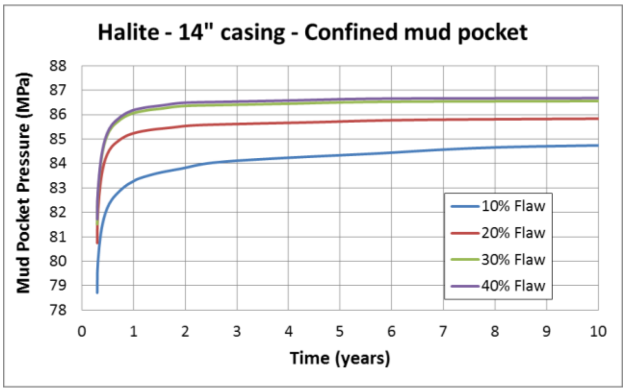

Figure 13. Yield index for 14" casing and Carnalite over time.

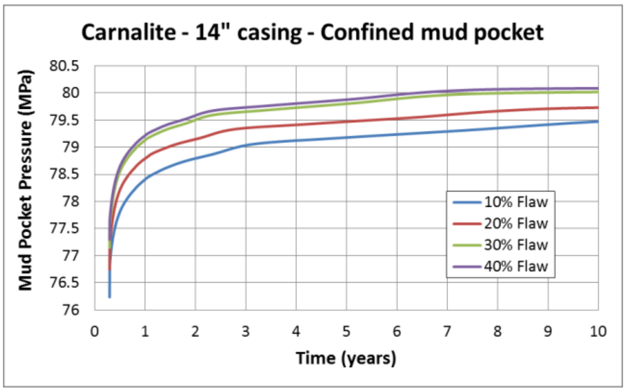

Figure 14. Yield index for 14" casing and Carnalite over time.

Figure 15 compares casing deformation for Carnalite rock and 30% mud pocket with (a) and without (b) fluid compressibility effects. It is clear that fluid compressibility counteracts pipe and rock deformation, reducing pressure non uniformity over casing surface.

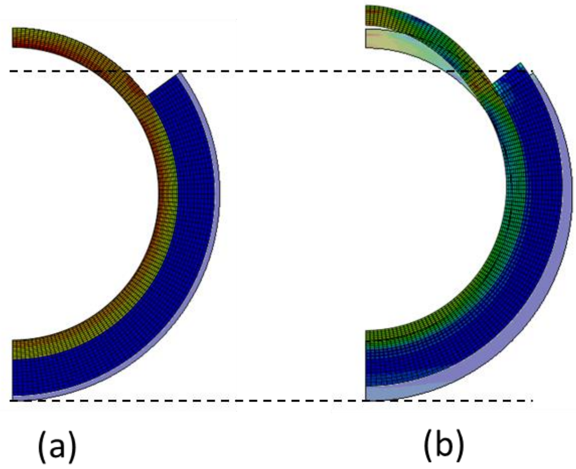

Figure 15. Comparison of casing and cement deformation for mud pocket of a) 10%, b) 20%, c) 30% and d) 40%, based on Carnalite rock.

5 CONCLUSION

The present work focused on the investigation of casing failure for a variety of cement defects, considering its connectivity to the rest of the annular. Results show that connected mud pockets offer a higher load discontinuity over casing wall, generating non uniform loads that can lead to casing failure.

For confined fluid, its expansion combined with volume reduction due to salt creep counteracts casing deformation, reducing significantly von Mises stress in the pipe. For confined flaws, Salt properties have an important impact. Higher mobility rocks tend to equilibrate fluid pressure with overburden stress and absorb (deform) any pressure increase over that stress. On the other hand, low mobility salts transfer the pressure above overburden stress to the casing.

Last but not least, casing deformation is more severe for 30% defects due to its free wall critical length. As the defect approaches 50% of the wellbore, rigid body displacement increases, reducing pipe's local buckle.

NOMENCLATURE

σ_1	First principal stress
σ_2	Second principal stress
σ_3	Third principal stress
t	Time
s_y	Yield stress
$\dot{\varepsilon}$	Strain rate
$\dot{\varepsilon}_0$	Reference strain rate
$\tilde{q}$	von Mises stress(Differential stress)
s_0	Reference stress
Q	Activation energy = 12Kcal/mol
R	Universal gas constant = 1.9858e-3 Kcal/mol K
q_0	Reference temperature
q	Temperature
K	Bulk modulus
V_0	Initial cavity volume
P	Pressure
V	Volume
a	Thermal expansion

REFERENCES

Jammer, P.; Hariharan, H.; Klever, F.J. (2015) Casing Collapse Strength Enhancement Due to Cement and Pipe Support via Modelling and Testing, *SPE 173069* London, England, UK.

Mackey, F.E (2011) Analise Geomecânica na Perfuração e Cimentação de Poços de Petróleo em Zonas de Sal, *Tese de doutorado* Pontifícia Universidade Católica do Rio de Janeiro, RJ, Brazil.

Poaite, E.J. and Costa, A.M. (2006) Well Design for Drilling Through Thick Evapore Layers in Santos Basin, *SPE 99161*, Miami, FL, USA.

Poiate, E.J (2012) Mecânica das Rochas e Mecânica Computacional para projetos de Poços de Petróleo em Zonas de Sal, *Tese de doutorado* Pontifícia Universidade Católica do Rio de Janeiro, RJ, Brazil.

Santos, B.F (2006) Modificações Morfológicas e Estruturais de Pastas de Cimento Aditivadas com Termofixo a Base de Epoxi para a Utilização em Poços de Petróleo, *Dissertação de mestrado* Universidade Federal de Sergipe, São Cristóvão, Brazil.

Thomas, J et al (2001) Fundamentos de Engenharia de Petróleo, *Editora Interciência* PETROBRAS, Rio de Janeiro, Brazil, Vol. 1, p. 142.

Timoshenko, S.; J.M. Gere. (1961) Theory of elastic stability, 2nd. ed., New York: MacGraw-Hill Book Company.

Zhang, J. and Standfird, W. (2008) Casing Ultradeep, Ultralong Salt Sections in Deep Water: A Case Study for Failure Diagnosis and Risk Mitigation in Record Depth Well, *SPE 114273* IFAI, Denver, Col, USA.